Climatic Change (2008) 87:361–383
DOI 10.1007/s10584-007-9317-5

# The relationship between climate and outbreak characteristics of the spruce budworm in eastern Canada

**David R. Gray**

Received: 5 May 2005 / Accepted: 27 June 2007 / Published online: 11 September 2007


**Abstract** The relationship between outbreak characteristics of the spruce budworm and the combination of climate, forest composition, and spatial location was examined in eastern Canada by the method of constrained ordination. Approximately 54% of the spatial variability in outbreak pattern, as described by a matrix of four outbreak characteristics, was explained by the spatial pattern of the climate (a matrix of six variables), forest composition (a matrix of seven variables), and spatial location (a matrix of two variables). The relationships between outbreak variables and climate variables were highlighted, and future outbreak characteristics of the spruce budworm were projected using simulations of a global circulation model for the period 2081–2100 where $CO_2$ concentrations reach a maximum of approximately 550 ppm. Future outbreaks are predicted to be an average of approximately 6 years longer with an average of 15% greater defoliation. The methodology is described and the potential effects of climate change on landscape-scale outbreaks of the insect are discussed.

## 1 Introduction

The eastern spruce budworm, *Choristoneura fumiferana* Clem. (Lepidoptera: Tortricidae), is arguably the most damaging forest insect in North America's forest (Hardy et al. 1983). In Canada, this native insect occurs throughout most of the range of white spruce [*Picea glauca* (Moench) Voss] where its preferred host is balsam fir (*Abies balsamea* L. Mill.; Royama 1984). As a result of their vast spatial extent (Hardy et al. 1986) and impact, spruce budworm outbreaks are perhaps the major natural disturbance in Canada's boreal forest (Fleming 2000; Fleming et al. 2002). Population densities of this native defoliator have exhibited a somewhat regular, approximately 30–40 year cycle over an extensive landscape for at least the last three centuries (Royama 1984, 1992). During periods of population abundance (outbreaks), a few hundred larvae may be found on a single host branch. Between these outbreak periods, populations may be so low as to make it difficult

D. R. Gray (✉)
Natural Resources Canada, Canadian Forest Service – Atlantic Forestry Centre,
P.O. Box 4000, Fredericton, NB E3B 5P7, Canada
e-mail: dgray@nrcan.gc.ca

to find a single larva among several hundred branches (Royama 1992). Outbreaks occur somewhat synchronously over extensive areas (Royama 1984; Candau et al. 1998; Gray et al. 1999; Williams and Liebhold 2000), but outbreak duration varies regionally from as few as one to as many as 20 years (Candau et al. 1998; Gray et al. 1999).

Complete defoliation of the current year's needles of balsam fir can occur by the fourth year of an outbreak (Morris 1963), and tree mortality will begin by the fifth year (Belyea 1952). Spruce species [*P. glauca* (Moench.), *P. rubens* Sarg., and *P. mariana* (Mill.) B. S. P.] are also affected, although to a lesser degree (Greenbank 1963; Nealis and Régnière 2004). Radial growth can be reduced by as much as 75% after several years of severe defoliation (Miller 1977), and mortality has been extremely high in past outbreaks. Approximately 45% of the host trees in eastern Canada were killed during the outbreak of the 1910s–1920s (Swaine and Craighead 1924); mortality accounted for approximately 58% of the host volume in Ontario from 1943 to 1955 (Elliott 1960). Approximately one-half of all insect-caused losses in forest productivity in Canada has been attributed to spruce budworm (Hall and Moody 1994).

As a significant, landscape-scale disturbance event, spruce budworm outbreaks play an important role in the carbon flux in boreal forests (Kurz and Apps 1999; Fleming 2000). Boreal forest stands tend to be even aged, and progress from young, fast-growing, low-biomass stands that are rapid accumulators of carbon, to old, slow-growing, high-biomass stands that accumulate very little carbon. Defoliation during a spruce budworm outbreak reduces the rate of carbon accumulation by the host trees by reducing their growth. When an outbreak results in tree mortality, there is also an abrupt increase in the mass of dead organic matter from which carbon is transferred to the atmosphere through decomposition (Apps and Price 1996). Severe defoliation and tree mortality also temporarily increase the risk of forest fire (Fleming et al. 2002), which may result in a large transfer of carbon directly to the atmosphere (Cofer et al. 1996). Increasing concentrations of greenhouse gases (primarily $CO_2$) are a major cause of global warming (Brasseur et al. 2003). Conversely, severe outbreaks may also facilitate the replacement of an old, slow carbon-accumulating stand, with a young, rapid carbon-accumulating stand.

Several authors associated the initiation of an outbreak with several consecutive dry summers (Wellington et al. 1950; Greenbank 1956; Pilon and Blais 1961), or with spring and autumn droughts (Wellington et al. 1950; Ives 1974). Pilon and Blais (1961) supported the theory of "climatic release" (i.e., weather conditions allow the spruce budworm population to escape the factors that otherwise maintain it at an endemic level). Blais (1968) argued that forest conditions in Ontario and climatic conditions in the Atlantic provinces were the factors that limited outbreak occurrence. Wellington et al. (1950) demonstrated an association between June rainfall and amount of defoliation by spruce budworm, but a single site provided the evidence. In a more detailed examination of historic data from New Brunswick, Royama (1992) and Royama et al. (2005) refuted the direct role of climate in spruce budworm population oscillations. Conclusions were based on an intensive examination of mortality factors, and survival of large larvae was determined to be a principal factor in spruce budworm generation survival (Royama 1984) and, therefore, in spruce budworm population cycles. However, the study area constitutes less than 0.01% of the spruce budworm range, and processes that affect spatial variability in the natural enemies that influence spruce budworm generational survival, and hence in outbreak characteristics, could not be assessed.

Large spatial variation in the severity and duration of a spruce budworm outbreak do exist at the landscape level (Candau et al. 1998; Gray et al. 1999), and the potential role of climatic factors in influencing outbreak characteristics such as duration and severity has not

been investigated at this scale. The population dynamics system of the spruce budworm includes at least 25 parasites, hyperparasites, and disease agents (Huber et al. 1996), plus the three principle hosts and the insect itself. Temperature and/or precipitation have a demonstrated effect on each of these components of the system. Temperature and/or precipitation affect spruce budworm aggregation (Wellington 1949a, b), developmental rates (Régnière and You 1991; Weber et al. 1999), dispersal (Greenbank et al. 1980), feeding (Régnière and You 1991), fecundity (Sanders et al. 1978; Harvey 1983), and survival (Régnière and Duval 1998). Temperature and precipitation affect microsporidian parasite development (Wilson 1974), parasitoid developmental rates (Lysyk and Nealis 1988; Nealis and Fraser 1988; Thireau and Régnière 1995), flight activity (and presumably search rates; Elliott et al. 1986; Nyrop and Simmons 1986), longevity (Nealis and Fraser 1988), and oviposition rate (Nealis 1988). Temperature and precipitation also affect host phenology and growth (Lekas et al. 1990; Deslauriers et al. 2003), and epizootiology of forest insect pathogens (Smitley et al. 1995). However, it is not quantitatively known how all these components interact, nor what would be the net effect of these interacting components on the characteristics of spruce budworm outbreaks, in an altered climatic environment.

The very large range of spruce budworm, and the existence of long-term records of defoliation levels for most of this range, provide an opportunity to directly examine the relationship between climatic factors and spruce budworm outbreak characteristics at the landscape scale. The objectives of this paper are to: examine the spatial variability in the characteristics of a spruce budworm outbreak at the landscape scale; to identify climatic variables that are associated with that spatial variability; to quantify the relationship between the outbreak characteristics and climatic variables; and to project future outbreak characteristics that may result from climate change.

## 2 Materials and methods

It is assumed that spatial variability in the characteristics of a spruce budworm outbreak arises from three principal sources: (1) climatic conditions; (2) forest composition; (3) inherent spatial structure in outbreaks that may itself have several causes; plus an unexplained portion of the variability (error). To examine the relationship between these sources, the data describing the three sources must be compiled at a common spatial resolution. Of the three sources, the forest composition data are the most limiting, and 30,000 ha was selected as the common resolution (cell size) at which each data set would be compiled. A total of 4,744 square cells (30,000 ha each) were placed in a uniform grid pattern starting from the Manitoba–Ontario border (Fig. 1), and the climatic conditions, forest composition and spruce budworm outbreak characteristics were summarized within each cell.

### 2.1 Forest composition

Operational forest inventories in Canada are compiled by numerous agencies and forest industry representatives according to individual standards and formats. A national inventory with a uniform format (the Canadian Forest Inventory, hereafter CanFI) was compiled by Gray and Power (1997), and the 11,321 mapsheets that cover the approximately 1.7 million $km^2$ of eastern Canada (east of the Manitoba–Ontario border) were used in this study. The CanFI data are composed of individual records (which roughly correspond to individual forest stands) whose geographic locations are recorded as the mapsheet within which they

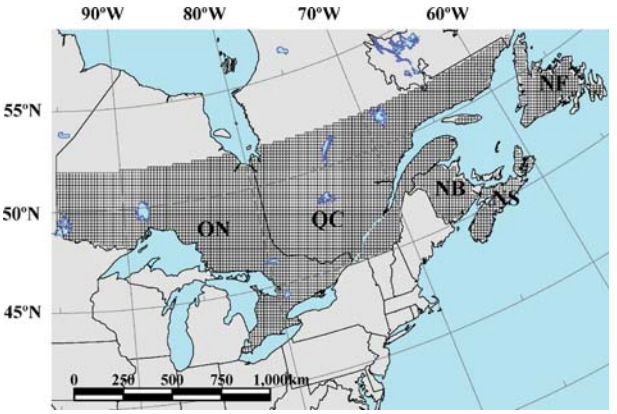


**Fig. 1** The 4,744 cells (30 000 ha) in which forest composition, climate variables, and spruce budworm outbreak characteristics were summarized

occur. Mapsheets vary in size across Canada ($\mu$=175 km$^2$; $\sigma$=324 km$^2$) and each mapsheet may contain many hundreds of records. A composite forest type was estimated for each mapsheet by summarizing each record according to the 10 species types listed in Table 1 The volume per ha (m$^3$/ha) of each species type, the forested area (ha), and the total area (ha) were calculated for each mapsheet.

The CanFI mapsheets were spatially intersected with the 30,000 ha cells, using the geographic information system ARC-Info (ESRI 2006). Average volumes (m$^3$/ha) of each species type were calculated for each cell using the volumes of each species type within each mapsheet, and the area of each mapsheet that intersected the cell. Forested area of each cell was calculated in a similar manner, and the forested proportion of each 30,000 ha cell was transformed ($for = \arcsin\left(\sqrt{\text{forested area}/30,000\text{ ha}}\right)$).

## 2.2 Spruce budworm outbreak characteristics

The provinces of Canada conduct annual surveys of forest insect damage from fixed-wing aircraft. Although surveys are done according to provincial protocols, the methodologies vary only slightly. In-flight surveyors use topographic maps to delineate polygons of insect damage and, in the case of spruce budworm, assign classes to their estimates of current-year defoliation within each polygon. MacLean and MacKinnon (1996) found the classification

**Table 1** Eleven species types compiled from the Canadian Forest Inventory

| Species type | Species |
|---|---|
| Black spruce | *Picea mariana* (Mill.) B. S. P. |
| Red/white spruce | *P. rubens* Sarg. &/or *P. glauca* (Moench) Voss |
| Balsam fir | *Abies balsamea* (L.) Mill. |
| White pine | *Pinus strobus* L. |
| Jack pine | *P. banksiana* Lamb |
| Red pine | *P. resinosa* Ait. |
| Eastern cedar | *Thuja occidentalis* L. |
| Other softwood | |
| Shade-tolerant hardwood[1] | |
| Shade-intolerant hardwood[1] | |

[1] (Harlow et al. 1979)

to be highly accurate. However, classification schemes vary among provinces, and over time within certain provinces. Therefore, in order to construct a uniform data set of defoliation records, broad defoliation classes ($C$) of '1' or '2' were assigned to the digitized defoliation polygons from 1941 to 1998, where the mid-points of the classes correspond to defoliation levels ($D$) of 20, and 65%, respectively. The forested area of Canada was covered with a grid of approximately 2×2 km cells (400 ha), and the digitized defoliation polygons from each year were intersected with the 2×2 km cells. The area of each 2×2 km cell that was outside the defoliation polygons was assigned the defoliation class $C$=0. One defoliation class ($C$) was assigned to each cell for each year according to the simple rule:

$$\begin{array}{c} \text{if } A_0 > A_1 + A_2 \text{ then } C = 0 \\ \text{else } C = C_{\max(A_1, A_2)} \end{array} \quad (1)$$

where $A_x$ is the area within the cell covered by the broad defoliation class $x$.

Defining the beginning and end of an outbreak is admittedly somewhat arbitrary in view of the fact that populations may undergo significant declines for 1 year in the midst of several years of otherwise high population levels. This can lead to a recorded defoliation level of zero in the middle of what most observers would consider a single multi-year outbreak. Therefore, for this study the last year of the most recent complete outbreak ($O_L$) from the 58-year period was defined in each 2×2 km cell as the most recent year with a non-zero $C$ followed by five consecutive values of $C$=0 (Gray et al. 1999). The first year of this most recent outbreak ($O_F$) was defined in each cell as the most recent year with a non-zero $C$ that preceded $O_L$, and was itself preceded by five consecutive values of $C$=0. Note that within a cell there may be some values where $C$=0 during the outbreak. The characteristics of this most recent outbreak are defined in each cell by *duration* ($O_L - O_F + 1$), *severity* ($\overline{D}_{O_F \text{ to } O_L}$) and *consistency* ($\sum_{i=O_F}^{O_L-1} \{1 - 0.5 \times |C_{i+1} - C_i|\} \Big/ (O_L - O_F)$). *Consistency* is a measure of the uniformity of defoliation levels during an outbreak. It counts the number of changes between successive values in the sequence of $C$s that defines the outbreak (a change from $C_t$=2 to $C_{t+1} = 0$ counting for two changes), and then scales the result to a maximum of 1 (i.e., completely consistent). *Consistency* is important because of its effect on host growth loss (see Section 4). The defoliation data were restricted to this most recent outbreak because older surveys were less spatially inclusive — therefore an area without a defoliation polygon could less reliably be assigned a defoliation class $C$=0.

A noticeable spatial trend in $O_F$ was removed by fitting a polynomial regression to $O_F$ using the stepwise option in the regression procedure of SAS (SAS Institute 1999). The residuals describe the number of years that $O_F$ pre-dated (negative *residual*) or post dated (positive *residual*) the predicted value of $O_F$. The means of *duration*, *severity*, *consistency*, and *residual* were calculated from the 2×2 km cell values within each 30,000 ha cell. Because *severity* and *consistency* are limited to values between 0 and 100%, and 0 and 1, respectively, they were transformed after the means were calculated within the 30,000 ha cells. The variables, *dur* ($\overline{\text{duration}}$), *sev* ($= \arcsin\left[\sqrt{\overline{\text{severity}}/100}\right]$), *con* ($= \arcsin\left[\sqrt{\overline{\text{consistency}}}\right]$), and *lag* ($\overline{\text{residual}}$) describe a spruce budworm outbreak within a 30,000 ha cell. The spatial variability in two of the characteristics of the outbreak are illustrated in Fig. 2a and c.

Following Hardy et al. (1986), it was assumed that aerial application of insecticides had little effect on outbreak characteristics in Ontario and Quebec at the resolution and scale used here. Candau et al. (1998) cite several sources when they note that less than 2% of the moderately to severely defoliated area was sprayed in the largest Ontario spray program. Analyses by Lysyk (1990) and Fleming et al. (1984) also reported aerial application did not result in a high level of foliage protection. However, in many years, aerial application of

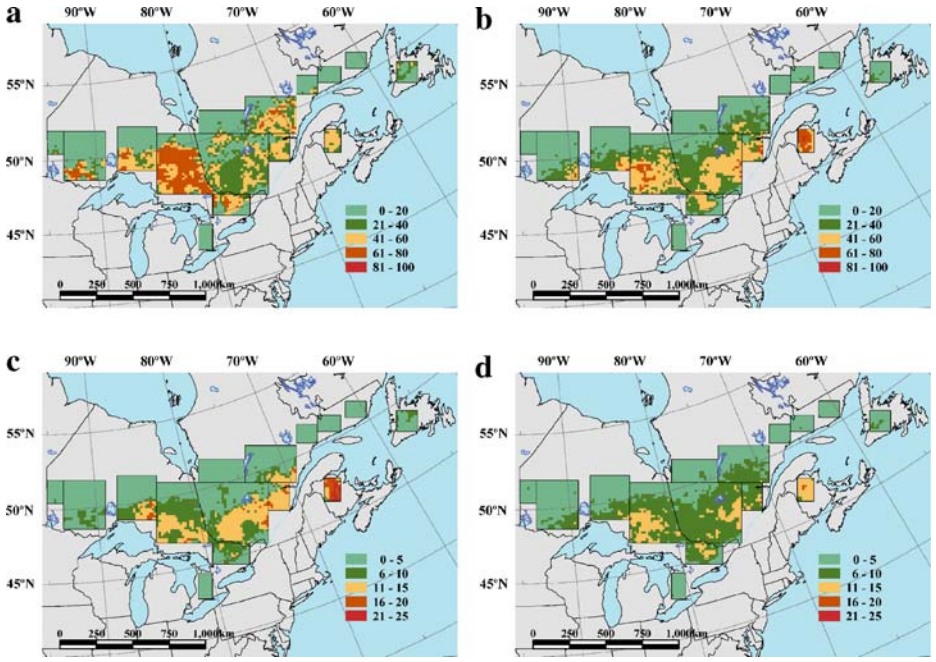


**Fig. 2** Historical observations, and model predictions, of outbreak severity (% defoliation) and duration (years) in the 3,245 cells used to build the model. Cells within each rectangular grid were permuted in Monte Carlo simulations for significance testing of explanatory variables. **a** observed severity; **b** predicted severity; **c** observed duration; **d** predicted duration

insecticides approached 50% of the moderately and severely infested areas in New Brunswick, and significant protection was achieved (Kettela 1995). Therefore, New Brunswick data were modified by increasing the observed provincial defoliation class by an amount representative of the mean foliage protection (Kettela 1995; Gray and MacKinnon 2007) obtained by the chemical *x* year combination.

### 2.3 Climatic characteristics

Average elevation of each 30,000 ha cell was estimated by intersecting the United States Geological Survey 30 arcsec Digital Elevation Model[1] (DEM) with the cells, and calculating the average elevation of the DEM values that fell within the cell.

The historic climate was derived from the 1961 to the 1990 Canadian Climate Normals database.[2] Daily weather variables were simulated from the normals for 20 years in each 30,000 ha cell using the stochastic weather generator of BioSIM (Régnière and Bolstad 1994; Régnière 1996). BioSIM simulates daily maximum (*Tx*) and minimum (*Tn*) temperatures (°C), and precipitation (*p*; mm) by matching georeferenced sources of weather data (the climate normals) to a grid of geographical coordinates (centroids of the 30,000 ha cells), adjusting the weather data for differences in latitude, longitude, and elevation between the source of weather data and each cell centroid. BioSIM restores

[1] http://edcdaac.usgs.gov/gtopo30/gtopo30.html

[2] Meteorological Service of Canada, Environment Canada

stochastic daily variation to the normals, while maintaining the autocorrelation between daily variables that occurs naturally (Régnière and Bolstad 1994).

From the 20 time series of daily weather generated in each cell, 13 historic climatic variables were chosen *a priori* to generally characterize the summer and winter climates that would be expected to influence insect survival, fecundity, search rates, etc. and disease development. Climate variables were calculated as follows, where subscripts *y*, *m*, and *d* refer to year, month, and day, respectively, and '.' indicates that the arithmetic operation was performed across all observations of that group. The variables are:

(1) sum of the average summer-monthly (April to August) extreme maximum temperatures over the 20 years,

$$s\_emax = \sum_{m=\text{April}}^{\text{August}} \left[ \frac{\sum_{y=1}^{20} \max\left(Tx_{ym\cdot}\right)}{20} \right] \quad ; \tag{2}$$

(2) sum of the average summer-monthly extreme minimum temperatures over the 20 years,

$$s\_emin = \sum_{m=\text{April}}^{\text{August}} \left[ \frac{\sum_{y=1}^{20} \min\left(Tn_{ym\cdot}\right)}{20} \right] \quad ; \tag{3}$$

(3) sum of the average summer-monthly mean maximum temperatures,

$$s\_mmax = \sum_{m=\text{April}}^{\text{August}} \overline{Tx_{\cdot m\cdot}} \quad ; \tag{4}$$

(4) sum of the average summer-monthly mean minimum temperatures,

$$s\_mmin = \sum_{m=\text{April}}^{\text{August}} \overline{Tn_{\cdot m\cdot}} \quad ; \tag{5}$$

(5) sum of the average winter-monthly (November to March) extreme maximum temperatures over the 20 years,

$$w\_emax = \sum_{m=\text{November}}^{\text{March}} \left[ \frac{\sum_{y=1}^{20} \max\left(Tx_{ym\cdot}\right)}{20} \right] \quad ; \tag{6}$$

(6) sum of the average winter-monthly (November to March) extreme minimum temperatures over the 20 years,

$$w\_emin = -\sum_{m=\text{Novemver}}^{\text{March}} \left[ \frac{\sum_{y=1}^{20} \min\left(Tn_{ym\cdot}\right)}{20} \right] \quad ; \tag{7}$$

(7) sum of the average winter-monthly mean maximum temperatures,

$$w\_mmax = \sum_{m=\text{January}}^{\text{December}} \overline{Tx_{\cdot m\cdot}} \quad ; \tag{8}$$

(8) sum of the average winter-monthly mean minimum temperatures,

$$w\_mmin = \sum_{m=\text{January}}^{\text{December}} \overline{Tn_{\cdot m \cdot}} \quad ; \tag{9}$$

(9) sum of the average summer-monthly total precipitation,

$$prec = \sum_{m=\text{April}}^{\text{August}} \overline{P_{\cdot m}} \quad ; \tag{10}$$

where $P$ is the total precipitation in a month);

10) sum of the average summer-monthly degree-days total,

$$s\_dd = \sum_{m=\text{April}}^{\text{August}} \overline{dd_{\cdot m}} \quad ; \tag{11}$$

where $dd$ is the total number of degree-days greater than 5°C in a month;

11) sum of the average winter-monthly winter-degree-days total,

$$w\_dd = \sum_{m=\text{November}}^{\text{March}} \overline{wd_{\cdot m}} \quad ; \tag{12}$$

where $wd$ is the total number of degree-days *below* −5°C in a month;

12) sum of the average summer-monthly vapor pressure deficits (mbar),

$$vpd = \sum_{m=\text{April}}^{\text{August}} \left\{ \frac{\sum_{y=1}^{20} 6.108 \sum_{d=1}^{n} \left[ 10^{\left( \frac{7.5 \times Tx_{ymd}}{237.3 + Tx_{ymd}} \right)} - 10^{\left( \frac{7.5 \times Tn_{ymd}}{237.3 + Tn_{ymd}} \right)} \right]}{20} \right\} \quad ; \tag{13}$$

13) sum of the average summer-monthly aridity index,

$$arid = \sum_{m=\text{April}}^{\text{August}} \max \left[ 0, \frac{\sum_{y=1}^{20} \left( PET_{ym} - P_{ym} \right)}{20} \right] \tag{14}$$

where $PET$ is Thornwaite's monthly potential evapotranspiration and $P$ is as above. The calculation of $vpd$ assumes that vapor pressure reaches saturation each day when $Tn$ is reached (usually at night), and that vapor gain or loss during the day is minimal (Murray 1967; Running et al. 1987). Monthly values of $PET_i$ were computed as in Dunne and Leopold (1978) using mean monthly air temperature as the only input.

Future climate projections (2081–2100) were obtained from the third Coupled Global Climate Model (CGCM3) of the Canadian Centre for Climate Modelling and Analysis.[3] The projected climate data used in this analysis were the daily atmospheric simulations produced by the IPCC SRES-B1 experiment in which $CO_2$ levels are stabilized at 550 ppm. The

[3] http://www.cccma.bc.ec.gc.ca/

CGCM3-B1 projections are at an approximately 2.81° latitude×2.81° longitude resolution. Climate normals were calculated from the 20-year weather trace at each grid node, and daily weather (2081–2100) was simulated for each 30,000 ha cell by BioSIM. Future climatic variables were estimated in the same manner as the historic climatic variables.

### 2.4 Model building

Constrained ordination (or canonical analysis) examines the relationship between a matrix **Y** (a set of response variables collected from $n$ samples) and a matrix **X** (a set of explanatory variables collected at the same $n$ samples; ter Braak 1994). In constrained ordination, the ordination axes (which are linear combinations of the response variables describing independent environmental gradients) are constrained to be combinations of the explanatory variables. Constrained ordination is thus a multivariate form of regression analysis (reduced rank regression). The response variables are modelled together, as a function of the combined explanatory variables (ter Braak 1994) using the regression model $\mathbf{Y} = \mathbf{XM} + \mathbf{E}$, where **M** is a $p \times q$ matrix (number of variables in **X**×number of variables in **Y**; ter Braak and Looman 1994). In this study, **Y** is the $n \times 4$ matrix of the spruce budworm outbreak characteristics, and **X** is initially the $n \times 26$ matrix of the 13 climatic variables ($\mathbf{X}_C$), the 11 forest composition variables ($\mathbf{X}_F$), and the 2 spatial variables ($\mathbf{X}_S$) that are the latitudinal and longitudinal coordinates of the 30,000 ha cells. The matix **X** was reduced during model building.

Model building was done by step-wise forward selection of explanatory variables with the software CANOCO (ter Braak and Šmilauer 2002). Tests of significance for each explanatory variable were estimated by a Monte Carlo simulation, and required that cells be arranged in a rectangular grid so that each simulation could be done on the data set after a random toroidal permutation of the **Y** matrix (Besag and Clifford 1989; ter Braak and Šmilauer 2002). The 4,744 30,000 ha cells do not constitute a rectangular grid without excessive loss of cells (due to the shape of the study area). Therefore, 3,245 cells in 14 rectangular grids were defined within the data set ($\mu$=232 cells/grid; $\sigma$=303 cells/grid) and toroidal permutations were done independently on the **Y** matrix in each grid. Five hundred permutations were done for each explanatory variable and variables were added to the model if they passed a significance criterion with a Bonferroni correction [$p<\alpha/v$, where $\alpha$=0.05 and $v$ is the number of variables in the forward selection; Lepš and Šmilauer 2003)]. The significance of the final model was similarly estimated by 500 Monte Carlo simulations.

Following the strategy of Borcard et al. (1992), the total variance in **Y** was partitioned among $\mathbf{X}_C$, $\mathbf{X}_F$, and $\mathbf{X}_S$ by performing a series of partial constrained ordination tests (Table 2). In partial constrained ordination, the variability in **Y** is first reduced by the amount explained by a covariable matrix (e.g., $\mathbf{X}_F$, $\mathbf{X}_S$ or their combination), and the residual variability is used in a constrained ordination with one of the other **X** sub-matrices (ter Braak 1988; Lepš and Šmilauer 2003). Variation partitioning was done on the model-building data set.

Results of ordination analyses are typically displayed by ordination diagrams, which, although more informative than tabular presentation, require more skill to interpret (ter Braak 1994). The interpretation depends partly on which analytical and scaling options are chosen within CANOCO (ter Braak and Šmilauer 2002). This study used the linear procedure (redundancy analysis), scaling emphasis was placed on correlations between variables of **Y**, and the outbreak characteristics scores were not post-transformed. The interpretation of regression biplots constructed from an analysis with these options is by the following rules (ter Braak 1994; ter Braak and Šmilauer ter Braak and Šmilauer 2002). The

**Table 2** Partial constrained ordinations tests performed, and the portion of variance in the spruce budworm outbreak matrix (**Y**) accounted for by each test

| Test number | Covariable matrix | Explanatory matrix | Variance attribution[1] |
|---|---|---|---|
| 1 | none | $\mathbf{X}_F$ | $a+b+d+f$ |
| 2 | none | $\mathbf{X}_S$ | $e+d+f+g$ |
| 3 | none | $\mathbf{X}_C$ | $b+c+f+g$ |
| 4 | $\mathbf{X}_C$ | $\mathbf{X}_F$ | $a+d$ |
| 5 | $\mathbf{X}_S$ | $\mathbf{X}_F$ | $a+b$ |
| 6 | $[\mathbf{X}_C\ \mathbf{X}_S]$ | $\mathbf{X}_F$ | $a$ |
| 7 | $\mathbf{X}_C$ | $\mathbf{X}_S$ | $d+e$ |
| 8 | $\mathbf{X}_F$ | $\mathbf{X}_S$ | $e+g$ |
| 9 | $[\mathbf{X}_C\ \mathbf{X}_F]$ | $\mathbf{X}_S$ | $e$ |
| 10 | $\mathbf{X}_S$ | $\mathbf{X}_C$ | $b+c$ |
| 11 | $\mathbf{X}_F$ | $\mathbf{X}_C$ | $c+g$ |
| 12 | $[\mathbf{X}_S\ \mathbf{X}_F]$ | $\mathbf{X}_C$ | $c$ |

[1] See Fig. 4.

correlation coefficient between variables of **Y** is approximated by the cosine of the angle between the arrows representing the **Y** variables. Therefore, outbreak characteristics that exhibit a large positive correlation will be represented by arrows pointing in the same direction; characteristics exhibiting a large negative correlation will be represented by arrows pointing in opposite directions. The length of an arrow representing a variable of **Y** or of **X** is an approximate value of the standard deviation of the variable. Redundancy analysis standardizes all variables to zero mean and unit variance. Therefore, longer response arrows indicate a greater contribution of that variable to describing the variability in the outbreak. Similarly, longer explanatory arrows indicate a greater effect on **Y**. The relationship between variables of **Y** and variables of **X** is seen by projecting a line at a right angle from an explanatory arrow to the head of a response arrow which indicates the amount of change in the explanatory variable (in terms of standard deviations) associated with a change of one standard deviation in the response variable. Variables have their average standardized values (0.0) at the origin and the arrows point in the direction of increasing values. Angles between arrows and lengths of arrows are only approximations because of the impossibility of accurately representing *n*-dimensional space (one dimension for each ordination axis) in two-dimensional print format. However, in cases where the third and higher ordination axes add little to the cumulative variance explained, the approximations are very close. Regression biplots relate the rate of change in **Y** per unit change in $x_j$ (a variable of **X**), assuming that the other variables of **X** are held constant [cf. correlation biplots, which assume that the other variables of **X** co-vary with $x_j$ in the way that they do in the data set (ter Braak 1986)]. Thus, regression biplots represent marginal effects.

Estimation of cell-level outbreak characteristics [using either the historic climate characteristics or those of the climate change projection (2081–2100)] is done in the following manner for each cell *i*.

(1) explanatory variables ($z_j$, $j$=1 to $p$) were each standardized by subtracting their mean and dividing by their standard deviation,

$$x_{ij} = \frac{z_{ij} - \bar{z}_j}{\sigma_j}; \tag{15}$$

(2) sample scores [*sensu* ter Braak and Šmilauer 2002] were calculated by multiplying the standardized variables (Eq. 15) by their respective first regression/canonical coefficients (produced as part of the CANOCO output) and summing the result,

$$x'_{i1} = \sum_{j=1}^{n} \left(x_{ij} \times c_{j1}\right), \tag{16}$$

and by their respective second regression/canonical coefficients (higher coefficients were not significant) and summing the result:

$$x'_{i2} = \sum_{j=1}^{n} \left(x_{ij} \times c_{j2}\right); \tag{17}$$

(3) the first and second sample scores (Eqs. 16 and 17, respectively) were multiplied by the two species scores (*sensu* ter Braak and Šmilauer 2002, and produced as part of the CANOCO output) of a response variable $k$, and summed,

$$\psi_{ik} = x'_{i1} \times b_{k1} + x'_{i2} \times b_{k2} \text{ for } k = 1 \text{ to } 4, \tag{18}$$

(4) the four standardized response variables (Eq. 18) were un-standardized by multiplying the standardized variable by the standard deviation of the response variable and adding its mean,

$$\widehat{y}_{ik} = \psi_{ik} \times \sigma_k + \overline{y}_k \quad , \tag{19}$$

(5) and outbreak variables *severity* and *consistency* were calculated by back transforming response variables $\widehat{y}_{i\,\mathrm{sev}}$ and $\widehat{y}_{i\,\mathrm{con}}$,

$$\widehat{y}_{i\,\mathrm{severity}} = \left[\sin\left(\psi_{i\,\mathrm{sev}} \times \sigma_{\mathrm{sev}} + \overline{y}_{\mathrm{sev}}\right)\right]^2 \times 100 \tag{20}$$

$$\widehat{y}_{i\,\mathrm{consistency}} = \left[\sin\left(\psi_{i\,\mathrm{con}} \times \sigma_{\mathrm{con}} + \overline{y}_{\mathrm{con}}\right)\right]^2 \quad . \tag{21}$$

## 3 Results

### 3.1 SBW outbreak

Approximately 63% of the spatial trend in $O_F$ (the first year of the spruce budworm outbreak) was explained by a polynomial function of geographic coordinates: $O_F = f(\mathrm{lon}, \mathrm{lat}, \mathrm{lon}^2, \mathrm{lon} \times \mathrm{lat}, \mathrm{lon}^3, \mathrm{lon}^2 \times \mathrm{lat}, \mathrm{lon} \times \mathrm{lat}^2, \mathrm{lat}^3)$. Parameter estimates and $F$ statistics are given in Table 3. The function removed the observed spatial trend in $O_F$ and a plot of residuals (equals the outbreak variable lag) did not show any particular bias with longitude or latitude (Fig. 3).

Considering only the 2×2 km cells with positive records of spruce budworm defoliation: the outbreak lasted an average of approximately 9 years; mean outbreak *severity* (i.e., the untransformed variable) was approximately 47%; and mean outbreak *consistency* (i.e., the untransformed variable) was approximately 0.7, which indicates that there was an average of more than four changes between consecutive defoliation classes during an average

**Table 3** Parameter estimates, standard errors and $F$ statistics associated with the polynomial function describing the spatial trend in $O_F$ (the first year of the spruce budworm outbreak)

| Variable name | Parameter estimate | $F$ value |
|---|---|---|
| *intercept* | 2,648.73213 | 3,558.21 |
| *lon* | 7.38636 | 64.20 |
| *lat* | −9.44705 | 50.46 |
| $lon^2$ | 0.13769 | 1,518.25 |
| $lon \times lat$ | 0.23845 | 45.86 |
| $lon^3$ | −0.00042521 | 4,359.67 |
| $lon^2 \times lat$ | −0.00438 | 3,480.32 |
| $lon \times lat^2$ | −0.00984 | 694.82 |
| $lat^3$ | −0.00255 | 176.52 |

All parameters were significant ($\alpha$<0.0001).

outbreak of 9 years (a change from $C_t$=2 to $C_{t+1} = 0$ counting for two changes). Outbreak duration was longest in New Brunswick ($\overline{x}_{dur} \approx 14$ y) and shortest in Newfoundland ($\overline{x}_{dur} \approx 6$ y). Outbreaks were most severe in Ontario ($\overline{x}_{sev} \approx 57\%$) and least severe in Newfoundland ($\overline{s}_{sev} \approx 34\%$). The characteristics of the outbreak calculated on the 2×2 km cells with positive defoliation records are shown for each province in Table 4.

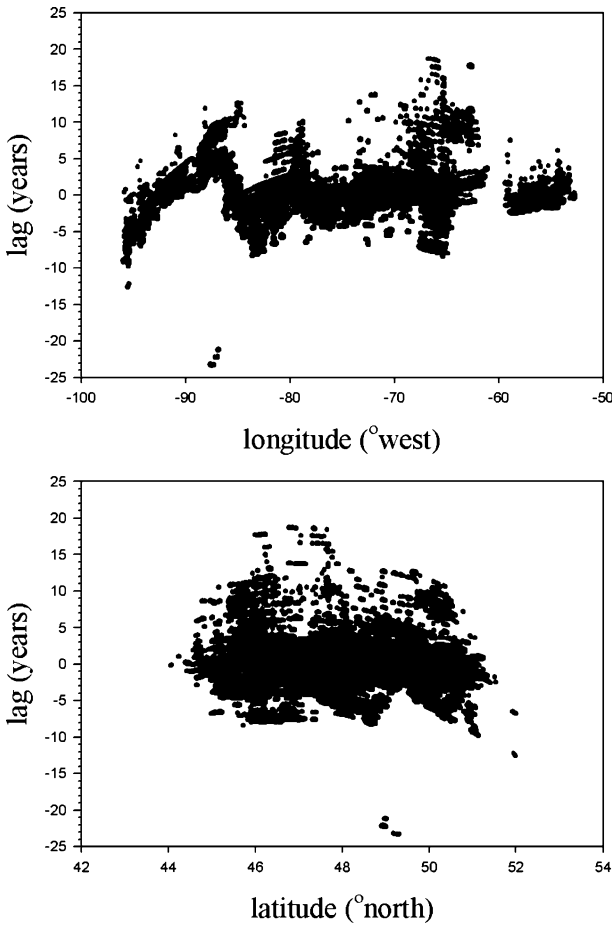


**Fig. 3** Relationship between the outbreak variable lag and longitude and latitude

**Table 4** Outbreak characteristics of the last spruce budworm outbreak in eastern Canada calculated from the 2×2 km cells with positive defoliation records: means and standard deviations

| Province | Number | Mean (and standard deviation) of outbreak characteristic | | | |
|---|---|---|---|---|---|
| | | lag (yr) | dur (yr) | *severity*[a] (%) | *consistency*[a] |
| Ontario | 76 252 | 0.06 (3.38) | 8.34 (3.49) | 57.16 (11.03) | 0.87 (0.19) |
| Quebec | 100 698 | 0.28 (2.01) | 9.04 (4.84) | 41.41 (13.39) | 0.69 (0.21) |
| New Brunswick | 15 953 | −1.93 (3.96) | 13.83 (5.99) | 39.84 (11.95) | 0.60 (0.17) |
| Newfoundland | 12 220 | −0.44 (1.13) | 5.70 (2.05) | 34.05 (13.83) | 0.70 (0.19) |
| Nova Scotia | 949 | 8.92 (1.15) | 3.47 (1.09) | 47.91 (14.23) | 0.60 (0.31) |
| Prince Edward Island | 234 | 11.91 (2.72) | 6.16 (3.04) | 32.15 (19.30) | 0.72 (0.22) |
| Combined | 206 306 | 0.04 (2.89) | 8.93 (4.66) | 46.69 (14.96) | 0.75 (0.22) |

[a] This is the untransformed variable.

## 3.2 Model building

Outbreak characteristics *duration, sev* and *con* were all highly correlated (>0.9), and contributed almost equally to variability in the last spruce budworm outbreak in eastern Canada (Table 5). The characteristic *lag* was less highly correlated with the other characteristics and contributed only approximately 1/2 to 1/3 as much as the other characteristics to outbreak variability (Table 5). Correlations, means, standard deviations and outbreak scores [≡ species scores *sensu* ter Braak and Šmilauer 2002] of the response variables used for estimating cell-level outbreak characteristics from the $\mathbf{Y} = \mathbf{XM} + \mathbf{E}$ model are shown in Table 5.

Fifteen of the 26 variables of $\mathbf{X}$ were estimated to be significant variables in the $\mathbf{Y} = \mathbf{XM} + \mathbf{E}$ model. Longitude (decimal-degrees west), latitude (decimal-degrees north), *s_emax*, *s_emin*, *s_mmin*, *w_emin*, *s_dd and arid* were significant ($\alpha$<0.05, with Bonferroni correction) climate variables in the model. Volume ($m^3$/ha) of black spruce, red/white spruce, balsam fir, eastern cedar, tolerant hardwood, intolerant hardwood and forested area were also significant ($\alpha$<0.05). Approximately 54% of the spatial variability in outbreak characteristics was explained by the matrix of significant explanatory variables.

**Table 5** Outbreak variables of the last spruce budworm outbreak calculated from the 30,000 ha cells for model building: correlations between; the relative contribution to the spatial variability in the last outbreak in eastern Canada; outbreak scores [≡ species scores *sensu* ter Braak and Šmilauer (2002)]; mean and standard deviations

| | dur | *sev*[a] | *con*[a] | lag |
|---|---|---|---|---|
| dur | | 0.988 | 0.973 | −0.403 |
| *sev*[a] | | | 0.997 | −0.259 |
| *con*[a] | | | | −0.181 |
| Relative contribution to outbreak variability | 2.27 | 1.94 | 1.65 | 1.00 |
| First outbreak score | −0.8095 | −0.7609 | −0.6412 | 0.1305 |
| Second outbreak score | 0.0622 | −0.0579 | −0.1011 | −0.3711 |
| Mean | 4.7506 | 25.6180 | 62.7928 | −0.2798 |
| Standard deviation | 5.1463 | 20.4069 | 16.1659 | 2.5376 |

[a] This is the transformed variable.

Means, standard deviations, and regression/canonical coefficients of the significant explanatory variables used for estimating cell-level outbreak characteristics from the $\mathbf{Y} = \mathbf{XM} + \mathbf{E}$ model are shown in Table 6. The $\mathbf{Y} = \mathbf{XM} + \mathbf{E}$ model was statistically significant ($\alpha < 0.002$); and the first two axes accounted for 96% of the relationship. Historical observations and model predictions of outbreak duration and severity are compared spatially in Fig. 2, where there is general agreement between observed and predicted values.

Partitioning the variance of $\mathbf{Y}$ between $\mathbf{X}_C$, $\mathbf{X}_F$ and $\mathbf{X}_S$ shows the degree to which climatic conditions and forest composition co-vary in a spatially similar manner. Approximately 25, 35, and 16% of the spatial variability in outbreak characteristics can be explained by the six climate, the seven forest composition, and the two spatial variables, respectively. However, portions of the explained variance in $\mathbf{Y}$ cannot be ascribed uniquely to any of $\mathbf{X}_C$, $\mathbf{X}_F$ or $\mathbf{X}_S$ because of similarities that exist in the spatial structures of the climate, forest, and location data (Fig. 4). The largest similarity in spatial structures occurred between the climate and forest, where approximately 12% of the variance in $\mathbf{Y}$ that can be explained by the climate variables could also be attributed to the forest composition (Fig. 4b). Similarly, 8% of the variance in $\mathbf{Y}$ than can be explained by the forest composition could also be attributed to the location variables (Fig. 4d). Results of the partitioning of the $\mathbf{Y}$ variance are illustrated in Fig. 4.

Summer degree-days (*s_dd*) has the strongest influence of the five significant climate variables on outbreak characteristics (Fig. 5). Using vector length as a measure of the marginal effect of each variable on the variance in outbreak characteristics (Fig. 5) indicates that *s_dd* has an 11× greater marginal effect than *arid* (the climate variable with the smallest marginal effect). Variables *s_mmin*, *s_emax*, *s_emin, and w_emin* have a 7×, 6×, 5× and 2× greater marginal effect, respectively, than *arid* on outbreak variability. Outbreak duration (*dur*) and severity (*sev*) are most affected by *s_dd* and *s_emax*: a 1 s.d. increase in *dur* (≈5 years) will occur with a 0.16 s.d. decrease in *s_dd* (equals 3 degree-days) or with a 0.28 s.d. increase in *s_emax*. The marginal effects of each climate variable on each outbreak variable are shown in Table 7.

**Table 6** Means, standard deviations and regression/canonical coefficients of the explanatory variables in the $Y = XM + E$ model

| Variable | Significance in $Y = XM + E$ Model | Mean | Standard deviation | First regression coefficient | Second regression coefficient |
|---|---|---|---|---|---|
| *for* | <0.002 | 49.8271 | 13.1431 | −0.3914 | 0.3633 |
| *north* | <0.002 | 49.0485 | 1.8838 | 0.8258 | 0.8450 |
| *r/wS* | <0.002 | 6.4344 | 5.0651 | −0.2146 | 0.2673 |
| *s_emin* | <0.002 | −16.4762 | 8.3457 | −1.2038 | −1.7826 |
| *TH* | <0.002 | 7.8984 | 15.8868 | 0.2171 | −0.3398 |
| *IH* | <0.002 | 28.2830 | 20.5263 | −0.1555 | −0.3851 |
| *arid* | <0.002 | 1.0808 | 3.5970 | 0.0098 | 0.4511 |
| *bS* | <0.002 | 41.5137 | 25.1083 | −0.0493 | −0.2220 |
| *bF* | =0.004 | 11.4433 | 10.3306 | −0.1483 | −0.6199 |
| *s_emax* | <0.002 | 121.1622 | 8.8727 | −2.5451 | 0.9832 |
| *s_dd* | <0.002 | 1,004.6622 | 182.6407 | 4.6019 | −1.6189 |
| *s_mmin* | <0.002 | 20.6990 | 7.6853 | −1.4749 | 2.9031 |
| *west* | <0.002 | 78.2176 | 8.3808 | 0.3250 | −1.0776 |
| *w_emin* | <0.002 | −149.8483 | 18.4545 | 0.8075 | 0.4387 |
| *eC* | <0.002 | 4.5269 | 6.2125 | −0.0550 | 0.6329 |

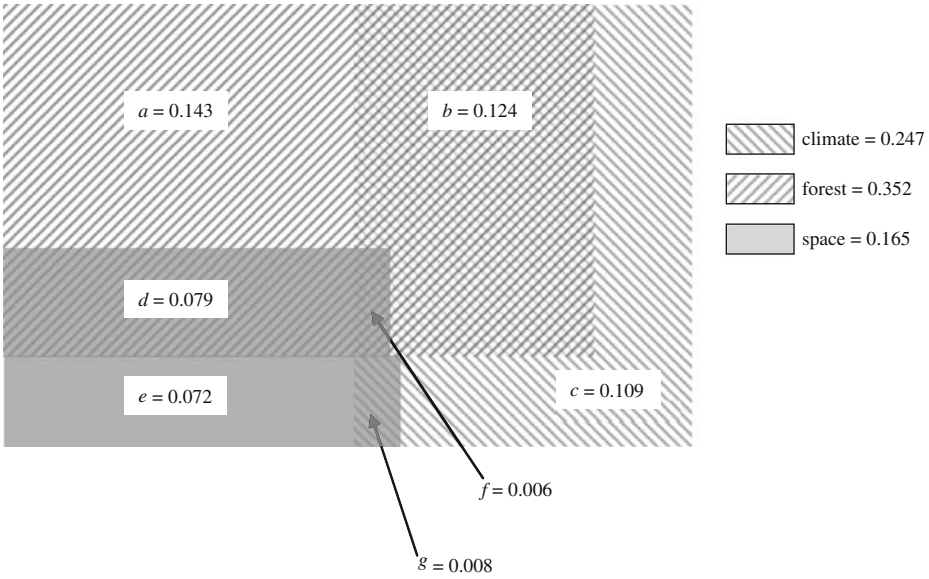


**Fig. 4** The partitioning of the variance in the matrix of spruce budworm outbreak characteristics. See Table 2 for a list of tests and variance components

### 3.3 Model projections

The future climate (2081–2100) is projected by the CGCM3-B1 scenario to be warmer and drier than the historical climate, although not uniformly so (Fig. 6a,b). The largest increase in *s_emax*, and *s_dd* are projected to occur in southern Ontario; the smallest increases are projected for Newfoundland. Mean projected changes in climate variables are shown in Table 8.

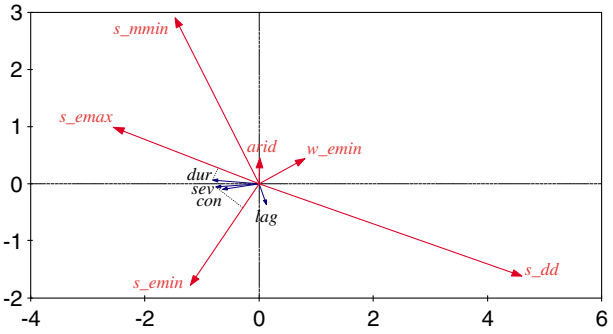


**Fig. 5** Regression biplot of the model where **Y** is the matrix of spruce budworm outbreak characteristics, and **X** is the combined matrix of significant climate variables, forest composition, and geographic location. For clarity, only the climate variables ($\mathbf{X}_C$) have been displayed. A regression biplot shows the rate of change in $y_k$ (a variable of **Y**) per unit change in $x_j$ (a variable of **X**) when the other variables of **X** are held constant. The change in *s_emax* or *s_emin* (proportion of 1 s.d.) necessary to produce a −1.0 s.d. change in *dur* and *sev*, respectively, are shown by the dotted lines that intersect the *s_emax* and *s_emin* vectors

**Table 7** Marginal effect of a 1 s.d. increase in the climate variables on outbreak variables in the $\mathbf{Y} = \mathbf{XM} + \mathbf{E}$ model

| | *dur* | *sev*[a] | *con*[a] | *lag*[b] |
|---|---|---|---|---|
| *s_emax* | 3.2184 | 3.2279 | 3.6321 | – |
| *s_emin* | 1.3102 | 1.7502 | 2.2564 | – |
| *s_mmin* | 2.0852 | 1.6386 | 1.5458 | – |
| *w_emin* | −0.9502 | −1.0987 | −1.3322 | – |
| *s_dd* | −5.8043 | −5.8521 | −6.6054 | – |
| *arid* | −0.0305 | −0.0577 | −0.1230 | – |

Changes in outbreak variables are given in units of s.d. of the outbreak variable.

[a] This is the transformed variable.

[b] See footnote 5

The following predictions of future outbreak characteristics under the future climate scenario are based on the marginal effects of the climate variables and assume that the forest composition remains constant. The average projected increase in s_emax of 7.9° [≈0.9× s.d. (Table 6)] is predicted to cause an increase in outbreak duration of approximately 15 years. However, the average increase in *s_dd* of 152 deg-days [≈0.8× s.d. (Table 6)] that is also projected by CGCM3-B1 is predicted to cause a decrease in

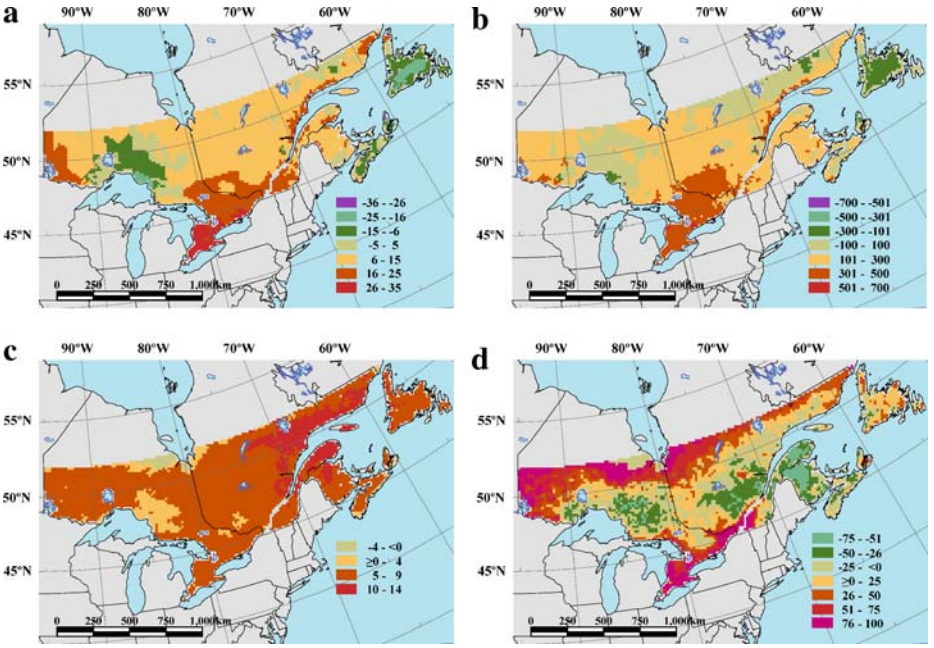


**Fig. 6** Projected changes (2081–2100 values minus historic values) in climate variables *s_emax* (°C) and *s_dd* (°C-day), and the predicted changes to spruce budworm outbreak duration (years) and severity (% defoliation; future model predictions minus historic model predictions). **a** predicted change in *s_emax*; **b** predicted change in *s_dd*; **c** predicted change in duration; **d** predicted change in severity

outbreak duration of approximately 25 years. The marginal effects of a change in a climate variable ($\Delta X_j$) on an outbreak variable ($\Delta Y_j$) can be calculated by

$$\Delta_{Y_k} = \frac{\Delta_{X_j}}{sd_{X_j}} \times b_{X_j Y_k} \times sd_{Y_k}, \tag{22}$$

where $sd_{X_j}$ and $sd_{Y_k}$ are the standard deviations of the historical climate variable $j$ (Table 6) and outbreak variable $k$ (Table 5), respectively, and $b_{X_j Y_k}$ is the relationship between $\mathbf{X}_j$ and $\mathbf{Y}_k$ (Table 7). The aggregate effect (i.e., sum of the marginal effects) of the projected future climate is predicted by the $\mathbf{Y} = \mathbf{XM} + \mathbf{E}$ model to result in an average increase in spruce budworm outbreak duration of approximately 6 years, an average increase in outbreak severity of 15%, and an average decrease in consistency of defoliation levels during an outbreak of 0.6 (Table 8[4]). The largest increases in outbreak duration are predicted for eastern Quebec and the Gaspé peninsula; the largest increases in outbreak severity are predicted for southern and northern Ontario. In spite of the average increase in outbreak severity, outbreak severity is predicted to decrease in large portions of eastern Canada under the future climate (Fig. 6).

## 4 Discussion

The northern limit to spruce budworm outbreaks in eastern Canada is south of approximately 52° N (Fig. 2a,b), whereas the range of its hosts extends well north of this latitude (Eyre and Ostrom 1965). Spruce budworm has been trapped as far north as 68° N (Volney and Fleming 2000). Hence, the northern limit to outbreaks does not appear to be directly related to the presence of its hosts nor to the presence of spruce budworm. However, outbreak characteristics are strongly related to climatic conditions (Fig. 5), and although there is no universally accepted definition of "outbreak," its detection at a landscape scale depends on a sufficiently large patch of sufficiently high defoliation to be observed by aerial survey. Predictions from the $\mathbf{Y} = \mathbf{XM} + \mathbf{E}$ model under the future climate scenario suggest that outbreak severity and duration will increase substantially in the northern portion of the study area (Fig. 6), suggesting that climate may be the factor that historically limits defoliation above 52° N to levels below what is detected as an outbreak. The geographic range of outbreaks is predicted to expand northward under the CGCM-B1 scenario.

Although higher values of all six significant climate variables are projected by the CGCM3-B1 scenario (Table 8), their marginal effects on spruce budworm outbreak duration and severity differ substantially (Fig. 5). For example, whereas the marginal effect of an increase in *s_emax* is to increase outbreak duration and severity, the marginal effect of an increase in *s_dd* or *w_emin* is to decrease duration and severity. This illustrates the complex nature of a system that includes more than 25 parasites, hyperparasites, and disease agents (Huber et al. 1996), in addition to the host and spruce budworm, which all may be uniquely influenced by seasonal weather.

[4] Predicted changes in the outbreak variable lag resulting from the projected climate of 2081–2100 are not included for consideration for the following reason. The outbreak variable lag is a residual from the spatial trend in first year of outbreak ($O_F$) – the number of years that the beginning of the outbreak predates or postdates the locally average beginning of the outbreak. Although the climate variables have been shown to have a significant effect on historical values of lag, the spatial variation in climate changes will tend to modify local lag values equally. In addition, it is likely that the spatial trend in $O_F$ will be altered by climate; therefore, predictions of residuals under a future climate are not possible.

**Table 8** Means and standard deviations (s.d.) of the changes in climate variables projected by CGCM3 (IPCC SRES-B1 experiment), and the means and standard deviations of the predicted outbreak variables from the Y = XM + E model

| Variable | Mean change | S.D. of change |
|---|---|---|
| *s_emax* | 7.9 | 9.7 |
| *s_emin* | 2.4 | 6.5 |
| *s_mmin* | 9.9 | 4.8 |
| *w_emin* | 25.6 | 16.4 |
| *s_dd* | 152.6 | 144.4 |
| *arid* | 264.9 | 29.7 |
| *duration* | 6.4 | 2.2 |
| *severity*[a] | 15.0 | 40.6 |
| *consistency*[a] | −0.6 | 0.4 |
| *lag*[b] | – | – |

Changes are calculated as 2081–2100 values minus historic values.

[a] This is the untransformed variable.

[b] See footnote 5

A spruce budworm outbreak begins when the biological forces contributing to a population increase exceed the forces contributing to a population decrease. The outbreak begins to collapse when the reverse is true. The generally higher daily summer temperatures (i.e., higher *s_dd*) may be of greater benefit to the natural enemy complex through increased developmental rate, fecundity, and search rate than to the spruce budworm through increased fecundity and survival. Higher summer extreme maximum temperatures (i.e., higher s_emax) may be disadvantageous to the natural enemies if the temperature extremes exceed the optimum temperatures for developmental rate.

It has been observed that gypsy moth populations may crash after a winter with a large number of days with mild temperatures (Roberts et al. 1993); and Gray (1994) suggested that the higher metabolic rates that accompany higher temperatures may deplete overwintering nutrient reserves. Higher winter extreme minimum temperatures (i.e., higher *w_emin*) may be of greater disadvantage to the natural enemies than to the spruce budworm through decreased overwintering survival. The decrease in the average consistency of defoliation levels during an outbreak (i.e., lower *consistency*) may be a result of an increase in the frequency of years with high overwintering mortality of natural enemies because of high *w_emin*. Cumulative defoliation values [the factor used to quantify the effect of a sequence of defoliation levels (MacLean et al. 2001)] are generally lower where outbreaks of equal average defoliation (*severity*) have lower *consistency*.

However, approximately 1/2 of the effect of the climate variables on spruce budworm outbreaks may operate indirectly through their effect on forest composition. Approximately 24.7% of the variance in outbreak characteristics can be explained by climate, and approximately 12.4% of the variance (or 1/2 of the 24.7%) could also be attributed to forest composition (Fig. 4). A similarity in the spatial structure of climate and forest composition is expected, and forest composition may affect spruce budworm outbreak characteristics by its influence on natural enemy populations. The hypothesis that forest diversity influences abundance of natural enemies (the "enemies hypothesis") has not received as much attention in forest ecosystems as in agricultural systems (Riihimäki et al. 2005), but significant evidence exists that stand composition is an important factor in spruce budworm mortality from natural enemies (Simmons et al. 1975; Kemp 1978; Cappuccino et al. 1998).

These projected changes in spruce budworm outbreak characteristics cannot be easily translated as increases, or decreases, in the net carbon sequestered in Canada's boreal forest, nor into estimated changes in the carbon fluxes. More severe outbreaks of a longer duration will result in lower growth and higher mortality rates of the host trees, and higher production of small dead organic matter (needles). Higher mortality will increase the

replacement of old, large biomass, slow carbon-accumulating trees with young, small biomass, rapid carbon-accumulating trees.. Thus the present forest age structure, and that of the future forest, are critical in determining how a change in outbreak characteristics will shift the carbon flux. Clearcut harvesting (the predominant method in Canada) is the most important agent in altering the forest age structure. Because Canada harvests each year a volume approximately equal to twice the volume lost annually to all insect pests (Sterner and Davidson 1982), long-term harvesting patterns will be a dominant factor, in conjunction with spruce budworm outbreaks, that determine carbon fluxes.

The climate during the last spruce budworm outbreak has been generalized by the average conditions estimated by simulated daily weather of 1961–1990 regardless of when during this period the outbreak was observed in each 2×2 km cell. This is acceptable when one considers that an outbreak is just a phase of the cyclic dynamic of spruce budworm populations and that climate will exercise some influence throughout the cycle. On the other hand it was not possible to estimate an average forest composition from yearly forest inventories during the same time period because yearly inventories do not exist. Instead, a single inventory has been used to represent the forest compositions that were admittedly not temporally invariant. However, the relatively large size of a CanFI mapsheet, in which the inventory is summarized, will tend to dampen the finer scale changes in forest composition that occurred from harvesting during the time period covered by the spruce budworm outbreak. The 30,000 ha cell size at which this analysis was conducted will further dampen the fine scale changes in forest composition. For these reasons, the use of a temporally invariant forest composition is considered acceptable.

This analysis assumes that climate change will not, in the short term, cause such a disruption in the ecosystem structure as to disable the interactions between the host and pest components of the ecosystem. Fleming (1996) presents a model where, in a climate-warmed environment, the co-occurrence of a spruce budworm outbreak and a shifted ratio of regeneration vs. senescence rates of the host trees could so devastate the host population that it falls below a critical threshold, leading to fragmentation of the host. In such a scenario, increased spruce budworm mortality during moth dispersal would make future outbreaks less likely. This analysis suggests that outbreaks are, in fact, likely to become longer and more severe, particularly in the southern region of the system that is most susceptible under the hypothetical mechanism that Fleming (1996) describes. Under Fleming's model, the longer and more severe future outbreaks predicted by this analysis, will increase the probability of ecosystem disruption. Such a disruption would then make subsequent outbreaks less likely at the scales detected by aerial surveys.

This analysis has not attempted to address three other issues of importance in estimating future outbreak characteristics: changes in outbreak frequency (cycle periodicity); shifts in the current ranges of any of the components of the ecosystem; and natural selection, which, operating under a changed climate, may alter the interactions between spruce budworm and its environment. Regarding the first issue, Blais (1983) concluded that outbreaks have increased in frequency and duration in the 20th century. He proposed harvesting practices, fire protection, and insecticide use as likely causes for the increase. However, Candau et al. (1998) reported that there was no evidence of an increase in the cycle periodicity in Ontario, despite the general warming that has occurred over the last century. However, their analysis is hampered by the relatively short time series available for analysis (less than three complete cycles). More recently, Boulanger and Arsenault (2004) used timber from historic buildings as well as old-growth forests in a tree-ring analysis, and concluded that there has been no change in oubreak frequency. Regarding the second issue, the majority of analyses examining the potential effects of climate change on species ranges rely on the climate

envelope approach, whereby the current distribution is mapped, climatic indicators of the distribution are chosen, and the future distribution is mapped according to the projected spatial changes in the climatic indicators. The result is usually a prediction of range expansion. Davis et al. (1998) demonstrate why such an approach is misleading; and Thomas et al. (2001) suggest that both evolutionary and ecological processes respond to climate change and cause range shifts. The issue of shifting range in response to climate change is far from clear. For this reason, the projected changes in spruce budworm outbreak characteristics have been spatially limited to its historical range (Fig. 2a,b). However, the predicted increases in outbreak duration and severity, particularly at the northern portions of the study area, suggest that range expansion will also occur under the future climate projected by the CGCM3-B1 scenario if climate-induced changes in forest composition do not offset the increases. Regarding the last issue, it is highly likely that natural selection will cause a shift in genotypic frequencies in the spruce budworm under the pressure of a changing climate. Large outbreaks may contain as many as $7.2\times10^{15}$ insects (Fleming 1996) – a vast pool of potential genetic variation. It is beyond the scope of this work to examine the potential shift in genotype, and subsequent behavior, resulting from climate change.

Nonetheless, this analysis provides important information on the changes in spruce budworm outbreak characteristics that are likely to occur as a result of a projected change in Canada's climate through an analysis that simultaneously considers the climatic characteristics and forest composition that co-vary in a spatially similar manner. Future work will more fully examine the role of forest composition on outbreak characteristics, and simulation exercises will examine the potential net outcomes of climate change on outbreak characteristics and carbon sequestration.

**Acknowledgments** I thank Drs. Richard Fleming, Jan Volney, Barry Cooke and Jodi Braine for their critical reviews of earlier versions of this manuscript, two anonymous reviewers whose comments greatly improved the manuscript, and Wayne MacKinnon and Mark Budd for their assistance with data preparation and figures. This research was supported by the Natural Resources Canada Program of Energy Research and Development POL No. 6.1.1.

## References

Apps MJ, Price DT (1996) Introduction. In: Apps MJ, Price DT (eds) Forest ecosystems, forest management and the global carbon cycle. Springer, Heidelberg, Germany, pp 19–24

Belyea RM (1952) Death and deterioration of balsam fir weakened by spruce budworm defoliation in Ontario. Part II. An assessment of the role of associated insect species in the death of severely weakened trees. J For 50:729–738

Besag J, Clifford P (1989) Generalized Monte Carlo significance tests. Biometrika 76:633–642

Blais JR (1968) Regional variation in susceptibility of eastern North American forests to budworm attack based on history of outbreaks. For Chron 44:17–23

Blais JR (1983) Trends in the frequency, extent, and severity of spruce budworm outbreaks in Eastern Canada. Can J For Res 13:539–547

Borcard D, Legendre P, Drapeau P (1992) Partialling out the spatial component of ecological variation. Ecology 73:1045–1055

Boulanger Y, Arsenault D (2004) Spruce budworm outbreaks in Eastern Quebec over the last 450 years. Can J For Res 34:1035–1043

Brasseur GP, Prinn RG, Pszenny AP (2003) Atmospheric chemistry in a changing world: an integration and synthesis of a decade of tropospheric chemistry research. Springer, New York, USA, p 300

Candau J-N, Fleming RA, Hopkin A (1998) Spatiotemporal patterns of large-scale defoliation caused by the spruce budworm in Ontario since 1941. Can J For Res 28:1733–1741

Cappuccino N, Lavertu D, Bergeron Y, Régnière J (1998) Spruce budworm impact, abundance and parasitism rate in a patchy landscape. Oecologia 114:236–242

Cofer WRI, Winstead EL, Stocks BJ, Cahoon DR, Goldammer JG, Levine JS (1996) Composition of smoke from North American boreal forest fires. In: Goldammer JG, Furyaev VV (eds) Fire in ecosystems of boreal Eurasia. Kluwer, Dordrecht, pp 465–475

Davis AJ, Jenkinson LS, Lawton JH, Shorrocks B, Wood S (1998) Making mistakes when predicting shifts in species range in response to global warming. Nature 391:783–786

Deslauriers A, Morin H, Urbinati C, Carrer M (2003) Daily weather responses of balsam fir (*Abies balsamea* (L.) Mill.) stem radius increment from dendrometer analysis in the boreal forests of Québec (Canada). Trees 17:477–484

Dunne T, Leopold LB (1978) Water in environmental planning. Freeman, San Francisco, p 818

Elliott KR (1960) A history of recent infestations of the spruce budworm in North-Western Ontario, and an estimate of resultant timber losses. For Chron 36:61–82

Elliott NC, Simmons GA, Draper RJ (1986) Adult emergence and activity patterns of parasites of early instar jack pine budworm (Lepidoptera: Tortricidae). Environ Entomol 15:409–416

ESRI (2006) '*ARC-Info, ver. 9.2.*' Redlands, CA

Eyre FH, Ostrom CE (1965) Silvics of forest trees of the United States. Agriculture handbook. No. 271, United States Department of Agriculture, Forest Service

Fleming RA (1996) A mechanistic perspective of possible influences of climate change on defoliating insects in North America's boreal forest. Silva Fenn 30:281–294

Fleming RA (2000) Climate change and insect disturbance regimes in Canada's boreal forests. World Resour Rev 12:520–554

Fleming RA, Shoemaker CA, Stedinger JR (1984) An assessment of the impact of large scale spraying operations on the regional dynamics of spruce budworm (Lepidoptera: Tortricidae) populations. Can Entomol 116:633–644

Fleming RA, Candau J-N, McAlpine RS (2002) Landscape-scale analysis of interactions between insect defoliation and forest fire in Central Canada. Clim Change 55:251–272

Gray DR (1994) Gypsy moth development – a model of phenological events. PhD Dissertation. Virginia Polytechnic Institute and State University, Blacksburg, VA

Gray DR, MacKinnon WE (2007) Historical spruce budworm defoliation records adjusted for insecticide spraying in New Brunswick from 1965–1992. J Acadian Entomol Soc 3:1–6

Gray SL, Power K (1997) Canada's forest inventory 1991: the 1994 version – technical supplement. Information Report. BC-X-363, Natural Resouces Canada, Canadian Forest Service – Pacific Forestry Centre

Gray DR, Régnière J, Boulet B (1999) Analysis and use of historical patterns of spruce budworm defoliation to forecast outbreak patterns in Quebec. For Ecol Manag 127:217–231

Greenbank DO (1956) The role of climate and dispersal in the inititiation of outbreaks of the spruce budworm in New Brunswick. 1. The role of climate. Can J Zool 34:453–476

Greenbank DO (1963) Host species and the spruce budworm. Mem Entomol Soc Can 31:219–223

Greenbank DO, Schaefer GW, Rainey RC (1980) Spruce budworm (Lepidoptera: Tortricidae) moth flight and dispersal: new understanding from canopy observations, radar, and aircraft. Mem Entomol Soc Can 110:1–49

Hall JP, Moody BH (1994) Forest depletions caused by insects and diseases in Canada 1982–1987. Canadian Forest Service Information Report. ST-X-8

Hardy Y, Lafond A, Hamel L (1983) The epidemiology of the current spruce budworm outbreak in Quebec. For Sci 29:715–725

Hardy Y, Mainville M, Schmitt DM (1986) An atlas of spruce budworm defoliation in eastern North America, 1938–1980. Miscellaneous Publication 1449, United States Department of Agriculture, Forest Service, Washington, DC

Harlow WM, Harrar ES, White FM (1979) Textbook of dendrology. McGraw-Hill, New York

Harvey GT (1983) Environmental and genetic effects on mean egg weight in spruce budworm (Lepidoptera: Tortricidae). Can Entomol 115:1109–1117

Huber JT, Eveleigh ES, Pollock S, McCarthy P (1996) The chalcidoid parasitoids and hyperparasitoids (Hymenoptera: Chalcidoidea) of *Choristoneura* species (Lepidoptera: Tortricidae) in America North of Mexico. Can Entomol 128:1167–1220

Ives WGH (1974) Weather and outbreaks of the spruce budworm, Choristoneura fumiferana (Lepidoptera: Tortricidae). Information Report. NOR-X-118, Department of the Environment, Canadian Forestry Service – Northern Forest Research Centre

Kemp WP (1978) The influence of stand factors on parasitism of spruce budworm eggs by *Trichogramma minutum*. Environ Model Softw 7:685–688

Kettela EG (1995) Insect control in New Brunswick, 1974–1989. In: Armstrong JA, Ives WGH (eds) Forest insect pests in Canada. Natural Resources Canada – Canadian Forest Service, Ottawa, ON, Canada, pp 655–665

Kurz WA, Apps MJ (1999) A 70-year retrospective analysis of carbon fluxes in the Canadian forest sector. Ecol Appl 9:526–547

Lekas TM, MacDougal RG, MacLean DA, Thompson RG (1990) Seasonal trends and effects of temperature and rainfall on stem electrical capacitance of spruce and fir trees. Can J For Res 20:970–977
Lepš J, Šmilauer P (2003) Multivariate analysis of ecological data using CANOCO. Cambridge University Press, Cambridge, UK, p 269
Lysyk TJ (1990) Relationships between spruce budworm (Lepidoptera: Tortricidae) egg mass density and resultant defoliation of balsam fir and white spruce. Can Entomol 122:253–262
Lysyk TJ, Nealis VG (1988) Temperature requirements for development fo the jack pine budworm (Lepidoptera: Tortricidae) and two of its parasitoids (Hymenoptera). J Econ Entomol 81:1045–1051
MacLean DA, MacKinnon WE (1996) Accuracy of aerial sketch-mapping estimates of spruce budworm defoliation in New Brunswick. Can J For Res 26:2099–2108
MacLean DA, Erdle TA, MacKinnon WE, Porter KB, Beaton KP, Cormier G, Morehouse S, Budd M (2001) The spruce budworm decision support system: forest protection planning to sustain long-term wood supply. Can J For Res 31:1742–1757
Miller CA (1977) The feeding impact of spruce budworm on balsam fir. Can J For Res 7:76–84
Morris RF (1963) Foliage depletion and the spruce budworm. Mem Entomol Soc Can 31:223–227
Murray FW (1967) On the computation of saturation vapor pressure. J Appl Meteorol 6:203–204
Nealis VG (1988) Weather and the ecology of *Apanteles fumiferanae* Vier. (Hymenoptera: Braconidae). Mem Entomol Soc Can 146:57–70
Nealis VG, Fraser S (1988) Rate of development, reproduction, and mass-rearing of *Apanteles fumiferanae* Vier. (Hymenoptera: Braconidae) under controlled conditions. Can Entomol 120:197–204
Nealis VG, Régnière J (2004) Insect-host relationships influencing disturbance by the spruce budworm in a boreal mixedwood forest. Can J For Res 34:1870–1882
Nyrop JP, Simmons GA (1986) Temporal and spatial activity patterns of an adult parasitoid, *Glypta fumiferanae* (Hymenoptera: Ichneumonidae), and their influence on parasitism. Environ Entomol 15:481–487
Pilon JG, Blais JR (1961) Weather and outbreaks of the spruce budworm in the province of Quebec from 1939 to 1956. Can Entomol 63:118–123
Régnière J (1996) Generalized approach to landscape-wide seasonal forecasting with temperature-driven simulation models. Environ Entomol 25:869–881
Régnière J, Bolstad P (1994) Statistical simulation of daily air temperature patterns in eastern North America to forecast seasonal events in insect pest management. Environ Entomol 23:1368–1380
Régnière J, Duval P (1998) Overwintering mortality of spruce budworm, *Choristoneura fumiferana* (Clem.) (Lepidoptera: Tortricidae), populations under field conditions. Can Entomol 130:13–26
Régnière J, You M (1991) A simulation model of spruce budworm (Lepidoptera: Tortricidae) feeding on balsam fir and white spruce. Ecol Model 54:277–297
Riihimäki J, Kaitaniemi P, Koricheva J (2005) Testing the enemies hypothesis in forest stands: the important role of tree species composition. Oecologia 142:90–97
Roberts EA, Ravlin FW, Fleischer SJ (1993) Spatial data representation for integrated pest management programs. Am Entomol 39:92–107
Royama T (1984) Population dynamics of the spruce budworm. Ecol Monogr 54:429–462
Royama T (1992) Analytical population ecology. Chapman & Hall, London, UK, p 371
Royama T, MacKinnon WE, Kettela EG, Carter NE, Hartling LK (2005) Analysis of spruce budworm outbreak cycles in New Brunswick, Canada, since 1952. Ecology 86:1212–1224
Running SW, Nemani RR, Hungerford RD (1987) Extrapolation of synoptic meteorological data in mountainous terrain and its use for simulating forest evapotranspiration and photosynthesis. Can J For Res 17:472–483
Sanders CJ, Wallace DR, Lucuik GS (1978) Flight activity of female eastern spruce budworm (Lepidoptera: Tortricidae) at constant temperatures in the laboratory. Can Entomol 110:627–632
SAS Institute (1999) SAS/STAT® user's guide, version 8. SAS, Cary, NC, p 3884
Simmons GA, Leonard DE, Chen CW (1975) Influence of tree species density and composition on parasitism of the spruce budworm, *Choristoneura fumiferana*. Environ Entomol 4:832–836
Smitley DR, Bauer LS, Hajek AE, Sapio FJ, Humber RA (1995) Introduction and establishment of *Entomophaga maimaiga*, a fungal pathogen of gypsy moth (Lepidoptera: Lymantriidae) in Michigan. Environ Entomol 24:1685–1695
Sterner TE, Davidson AG (1982) Forest insect and disease conditions in Canada, 1981. Canadian Forest Service, Ottawa, ON
Swaine JM, Craighead FC (1924) Studies on the spruce budworm (*Cacoecia fumiferana* Clem.). Part I. A general account of the outbreaks, injury and associated insects. Technical Bulletin. 37, Department of Forestry, Ottawa
ter Braak CJF (1986) Canonical correspondence analysis: a new eigenvector technique for multivariate direct gradient analysis. Ecology 67:1167–1179

ter Braak CJF (1988) Partial canonical correspondence analysis. In: Bock HH (ed) Classification and related methods of data analysis. North Holland, Amsterdam, pp 551–558
ter Braak CJF (1994) Canonical community ordination. Part I: Basic theory and linear methods. Ecoscience 1:127–140
ter Braak CJF, Looman CWN (1994) Biplots in reduced-rank regression. Biom J 36:983–1003
ter Braak CJF, Šmilauer P (2002) Canoco reference manual and CanoDraw for Windows user's guide: software for canonical community ordination (version 4.5). in Microcomputer Power, Ithaca, NY
Thireau J-C, Régnière J (1995) Development, reproduction, voltinism and host synchrony of *Meteorus trachynotus* with its host *Choristoneura fumiferana* and *C. rosaceana*. Entomol Exp Appl 76:67–82
Thomas CD, Bodsworth EJ, Wilson RJ, Simmons AD, Davies ZG, Musche M, Conradt L (2001) Ecological and evolutionary processes at expanding range margins. Nature 411:577–581
Volney WJA, Fleming RA (2000) Climate change and impacts of boreal forest insects. Agric Ecosyst Environ 82:283–294
Weber JD, Volney WJA, SJR (1999) Intrinsic developmental rate of spruce budworm (Lepidoptera: Tortricidae) across a gradient of latitude. Environ Entomol 28:224–232
Wellington WG (1949a) The effects of temperature and moisture upon the behaviour of the spruce budworm, *Choristoneura fumiferana* Clemens (Lepidoptera: Tortricidae). I. The relative importance of graded temperatures and rates of evaporation in producing aggregations of larvae. Sci Agric 29:201–215
Wellington WG (1949b) The effects of temperature and moisture upon the behaviour of the spruce budworm, *Choristoneura fumiferana* Clemens (Lepidoptera: Tortricidae). II. The responses of larvae to gradients of evaporation. Sci Agric 29:216–229
Wellington WG, Fettes JJ, Turner KB, Belyea RM (1950) Physical and biological indicators of the development of outbreaks of the spruce budworm, *Choristoneura fumiferana* (Clem.) (Lepidoptera: Tortricidae). Can J Res Dev 28:308–331
Williams DW, Liebhold AM (2000) Spatial synchrony of spruce budworm outbreaks in eastern North America. Ecology 81:2753–2766
Wilson GG (1974) The effects of temperature and ultraviolet radiation on the infection of *Choristoneura fumiferana* and *Malacosoma pluviale* by a microsporidian parasite, *Nosema(Perezia) fumiferanae* (Thom.). Can J Zool 52:59–63